# Electronic Supporting Information (ESI)

# Photolysis, OH reactivity and ozone reactivity of a proxy for isoprene-derived hydroperoxyenals

Glenn M. Wolfe,[a] John D. Crounse,[b] Jonathan D. Parrish,[a] Jason M. St. Clair,[b] M. R. Beaver,[b,]* F. Paulot,[c] Tehshik P. Yoon,[a] Paul O. Wennberg,[b,d] and Frank N. Keutsch[a]

[a] Department of Chemistry, University of Wisconsin, Madison, Wisconsin 53706, USA.
[b] Division of Geological and Planetary Sciences, California Institute of Technology, Pasadena, California 91125, USA.
[c] Division of Engineering and Applied Sciences, Harvard University, Cambridge, MA 02138, USA.
[d] Division of Engineering and Applied Science, California Institute of Technology, Pasadena, California 91125, USA.
*now at: National Exposure Research Laboratory, US Environmental Protection Agency, Research Triangle Park, NC 27711, USA.

# 1 Synthesis of $C_6$-HPALD

**General Information.** Cobalt(II) 5,10,15,20-tetrakis(2,6-dichlorophenyl)porphyrin was prepared as previously described.[1, 2] $CH_2Cl_2$ was purified by elution through alumina as described by Pangborn et al..[3] *i*-PrOH was purified by distillation. All other reagents were purchased from commercial vendors and used without further purification.

**(2*E*,4*E*)-Hexa-2,4-dienal.** In a 100 mL round-bottomed flask was placed 3 g (30.57 mmol) sorbic alcohol in 53 mL $CH_2Cl_2$. The reaction was then cooled to 0 °C, and 16 g (184 mmol) activated $MnO_2$ was added. The reaction was allowed to warm to room temperature and stirred for 72 h. The black solid was removed by filtration, and the filtrate was concentrated by rotary evaporation at 0 °C to afford 2.55 g of a yellow oil (26.52 mmol, 87% yield). Spectral data for this material were identical to those previously reported.[4]

**(*E*)-4-Hydroperoxyhex-2-enal (C$_6$-HPALD).** Prepared as previously described by Sugamoto.[2] A solution of (2*E*,4*E*)-hexa-2,4-dienal (100 mg, 1.04 mmol) in a 5.2 mL mixture of 1:1 *i*-PrOH:$CH_2Cl_2$ was placed in a 15 mL vial. Co(tdcpp) (0.5 mg, 0.005 μmol) was added, and oxygen was bubbled through the solution for 2 min. A stopper equipped with an oxygen balloon was then attached to the vial, and $Et_3SiH$ (0.183 mL, 1.14 mmol) was added by syringe. The reaction was stirred for 2 h at room temperature. The reaction mixture was directly loaded onto a deactivated silica column and eluted using a gradient of 8:1 to 4:1 pentanes:acetone. The

hydroperoxide was isolated as 67.5 mg (0.52 mmol, 50% yield) of a yellow oil. Spectral data for this material were identical to those previously reported.[2] NMR spectra indicate an impurity of ~20% that can be ascribed to the singly-saturated and doubly-saturated alcohol analogues of the C6-HPALD (i.e. replacing –OOH with –OH), which are likely side-products of the second reaction step. These compounds are also present in the gas-phase as described in the main text.

## 2 CIMS $C_6$-HPALD Sensitivity and Identification

The CIMS sensitivity for $C_6$-HPALD was estimated from the calculated ion-molecule collision rate using the parameterization of Su and Chesnavich.[5] The average dipole moment and polarizibility of the molecule was determined via *ab initio* calculations at the B3LYP/cc-pVTZ level. Conformer-specific dipoles were calculated for all conformers with a relative population of >1% at T=298K, as estimated from a Boltzmann weighting to the conformer energies. The conformer-specific dipoles, weighted by their relative population, were then averaged to yield the overall dipole moment. This methodology is described in detail by Garden et al.[6] These calculations yield an average dipole moment of 3.6 D and a polarizability of 13.1 $Å^3$ for $C_6$-HPALD, from which we derive an ion-molecule collision rate for $C_6$-HPALD and the reagent ion ($CF_3O^-$) of 2.69 x $10^{-9}$ $cm^3$ $molecule^{-1}$ $s^{-1}$. From this value, the absolute sensitivity is determined by dividing by the $CF_3O^-$ + hydroxyacetone collision rate (2.4 x $10^{-9}$ $cm^3$ $molecule^{-1}$ $s^{-1}$), by the calibrated hydroxyacetone sensitivity (1.2 x $10^{-4}$ normalized counts $pptv^{-1}$).[7] The uncertainty in this calibration factor is conservatively estimated to be ±50% based on comparison of similarly calculated estimates with sensitivities derived from calibrations with authentic compounds.[7, 8]

The $C_6$-HPALD molecule was positively identified from CIMS measurements in three ways: 1) appearance of a signal at negative m/z 215 as expected for the cluster with $CF_3O^-$ (130 + 85), 2) an observed $^{13}C$-isotope at negative m/z 216 with the expected ratio to m/z 215 of ~7.7% (Fig. S1), and 3) The presence of the m/z 63 daughter ion in the tandem mass spectrum of m/z 215, which is a fingerprint for hydroperoxides (Fig. S2).[7, 9]

## 3 DHB Sensitivity

The CIMS sensitivity to dihydroxybenzene (DHB) could not be determined by standard additions, thus an alternative method was devised. The reaction chamber was filled with ~184 ppbv $CH_3ONO$ and ~2 ppmv phenol, and the lights were energized at the "low" setting to initiate OH oxidation of phenol, which forms DHB with a yield of 0.80 ± 0.12.[10] Both the phenol and DHB signals (m/z 180 and 129) were corrected for wall losses. The phenol signal was converted to concentrations with the calibrated sensitivity (see main text). DHB growth (in normalized counts) was corrected for the phenol reaction yield and for DHB loss via reaction with OH following Atkinson et al.[11]; the latter correction amounted to 1 – 10% of the total DHB signal. Finally, the slope of a plot of the corrected DHB signal versus phenol decay yields the estimated DHB sensitivity of 9.5 x $10^{-5}$ ncts $pptv^{-1}$ (Fig. S3). The uncertainty in this value is the sum of uncertainties from the linear fit (19%, $1\sigma$), the DHB yield (15%), the phenol calibration (5%) and wall losses (3%), giving a total estimated uncertainty of 42%.

## 4 Calculation of $C_6$-HPALD Photolysis Cross Section and Quantum Yield

The low vapor pressure of $C_6$-HPALD and the presence of low-volatility inorganic impurities prevent a direct experimental determination of the absorption cross section from gas-phase or condensed-phase UV-Visible spectroscopy. Thus, following the rationale that radiation is primarily absorbed by the O=C-C=C chromophore, we assume a cross section equal to the average of those measured for three molecules with the same chromophore (methacrolein,[12] acrolein[13] and (*E*)-2-hexenal[14, 15]).[16] The individual cross sections, as well as their average and standard deviation, are displayed in Fig. S4. This averaged value is used to calculate the quantum yield as described below.

Assuming a wavelength-independent quantum yield, the photolysis rate constant is given by

$$J = \phi \int \sigma(\lambda)I(\lambda)d\lambda \tag{1}$$

where $\phi$ is quantum yield, $\sigma$ is cross section, $\lambda$ is wavelength and I is photon flux. Integration of the product of this cross section and the measured light flux (also shown in Fig. S4) over the range 300 – 400 nm gives a value of $(6.0 \pm 1.6) \times 10^{-5}$ $s^{-1}$. Here, the $2\sigma$ uncertainty is calculated as the average of uncertainties in the cross section at each point weighted by the contribution of each point to the integrated rate constant. Substitution of the observed average $C_6$-HPALD photolysis rate constant of $(6.3 \pm 0.2) \times 10^{-5}$ $s^{-1}$ into the left-hand side of Eqn. (1) then allows us to solve for the "wavelength-averaged" quantum yield.

## References

1.     A. D. Adler, R. R. Longo, F. Kampas and J. Kim, *J. Inorg. Nucl. Chem.*, 1970, **32**, 2443-2445.
2.     K. Sugamoto, Y. Matsushita and T. Matsui, *J. Chem. Soc. Perkin Trans. 1*, 1998, **23**, 3989-3998.
3.     A. B. Pangborn, M. A. Giardello, R. H. Grubbs, R. K. Rosen and F. J. Timmers, *Organometallics*, 1996, **15**, 1518-1520.
4.     C. C. Cosner and P. Helquist, *Org. Lett.*, 2011, **13**, 2071-2073.
5.     T. Su and W. J. Chesnavich, *J. Chem. Phys.*, 1982, **76**, 5183-5185.
6.     A. L. Garden, F. Paulot, J. D. Crounse, I. J. Maxwell-Cameron, P. O. Wennberg and H. G. Kjaergaard, *Chem. Phys. Lett.*, 2009, **474**, 45-50.
7.     J. D. Crounse, F. Paulot, H. G. Kjaergaard and P. O. Wennberg, *Phys. Chem. Chem. Phys.*, 2011, **13**, 13607-13613.
8.     F. Paulot, J. D. Crounse, H. G. Kjaergaard, J. H. Kroll, J. H. Seinfeld and P. O. Wennberg, *Atmos. Chem. Phys.*, 2009, **9**, 1479-1501.
9.     F. Paulot, J. D. Crounse, H. G. Kjaergaard, A. Kurten, J. M. St Clair, J. H. Seinfeld and P. O. Wennberg, *Science*, 2009, **325**, 730-733.
10.    R. I. Olariu, B. Klotz, I. Barnes, K. H. Becker and R. Mocanu, *Atmos. Environ.*, 2002, **36**, 3685-3697.
11.    R. Atkinson, S. M. Aschmann, W. P. L. Carter, A. M. Winer and J. N. Pitts, *J. Phys. Chem.*, 1982, **86**, 4563-4569.
12.    T. Gierczak, J. B. Burkholder, R. K. Talukdar, A. Mellouki, S. B. Barone and A. R. Ravishankara, *J. Photochem. Photobiol. A: Chem.*, 1997, **110**, 1-10.
13.    I. Magneron, R. Thevenet, A. Mellouki, G. Le Bras, G. K. Moortgat and K. Wirtz, *J. Phys. Chem. A*, 2002, **106**, 2526-2537.
14.    E. Jimenez, B. Lanza, E. Martinez and J. Albaladejo, *Atmos. Chem. Phys.*, 2007, **7**, 1565-1574.

15. M. P. O'Connor, J. C. Wenger, A. Mellouki, K. Wirtz and A. Munoz, *Phys. Chem. Chem. Phys.*, 2006, **8**, 5236-5246.
16. H. Keller-Rudek and G. K. Moortgat, MPI-Mainz-UV-VIS Spectral Atlas of Gaseous Molecules, www.atmosphere.mpg.de/spectral-atlas-mainz, Accessed 03 March, 2012.
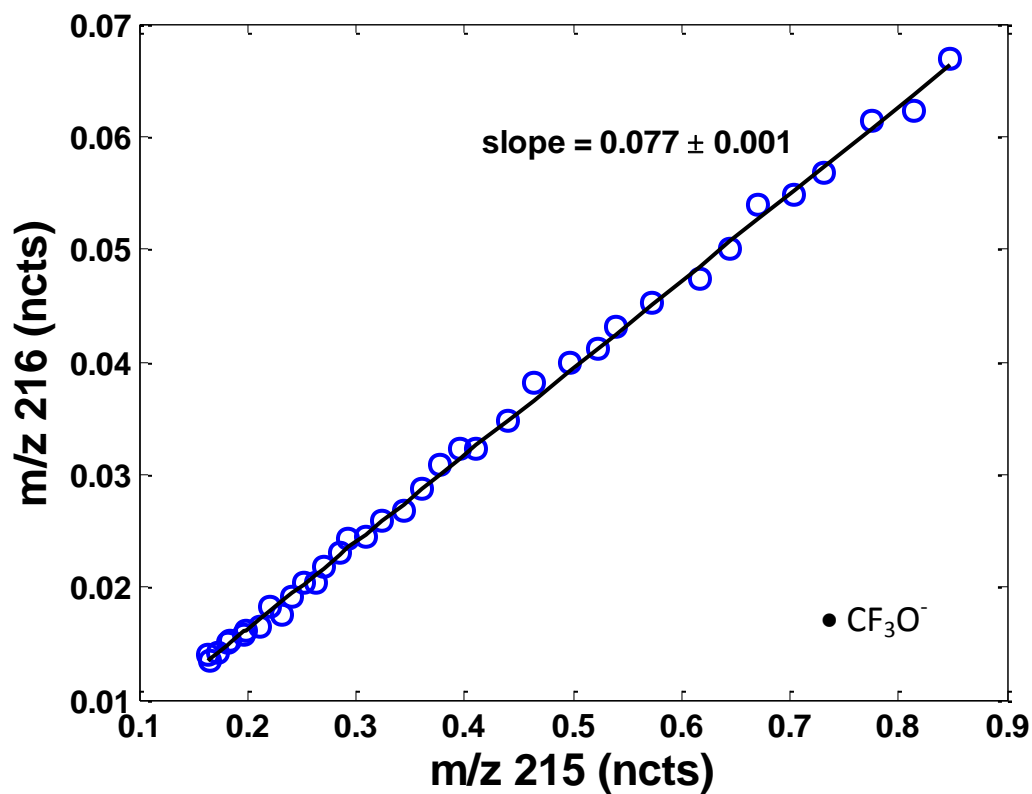17. J. Peeters and J. F. Müller, *Phys. Chem. Chem. Phys.*, 2010, **12**, 14227-14235.

**Figure S1.** Correlation of the $C_6$-HPALD cluster signal (m/z 215) with its $^{13}C$ isotope signal (m/z 216) for experiment OH1 (see Table 2 in main text). Units for both axes are reagent ion-normalized counts. The slope of 0.077 ± 0.001 corresponds to that expected for the 7-carbon ion.
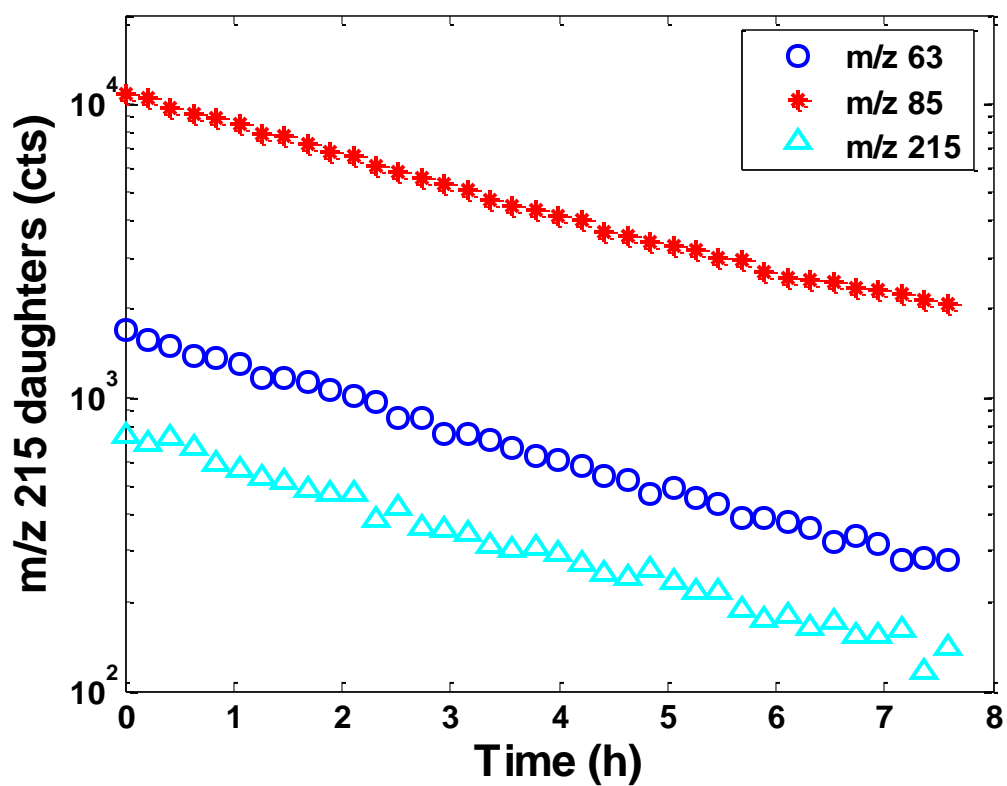
**Figure S2.** Time evolution of tandem MS daughter ions of negative m/z 215 for experiment OH1. Units are absolute counts. Signals correspond to the following daughter ions: $C_6$-HPALD·$CF_3O^-$ (m/z 215, light blue triangles), $CF_3O^-$ (m/z 85, red stars) and $FCO_2^-$ (m/z 63, blue circles). The latter is a marker for hydroperoxides.
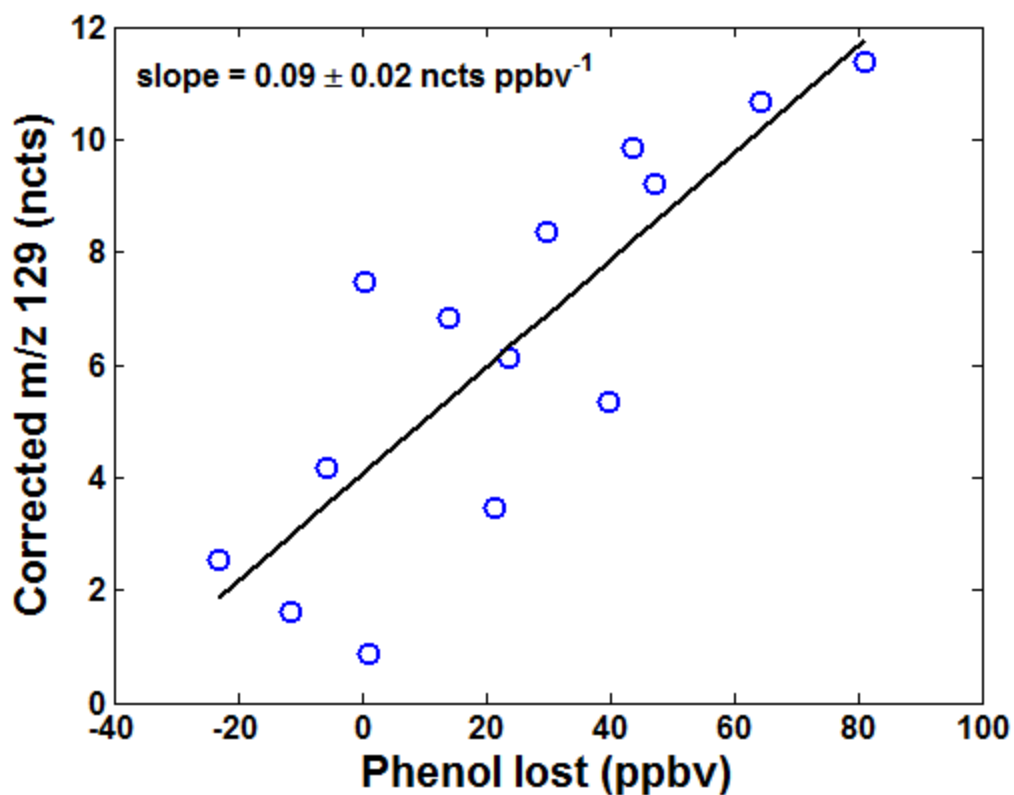
**Figure S3.** Calibration plot for DHB from the first 2 hours of the phenol OH oxidation experiment. The DHB signal (m/z 129) has been corrected for the phenol yield and loss to reaction with OH as described in the text. The line represents an ordinary linear least-squares fit, the slope of which represents the DHB sensitivity.
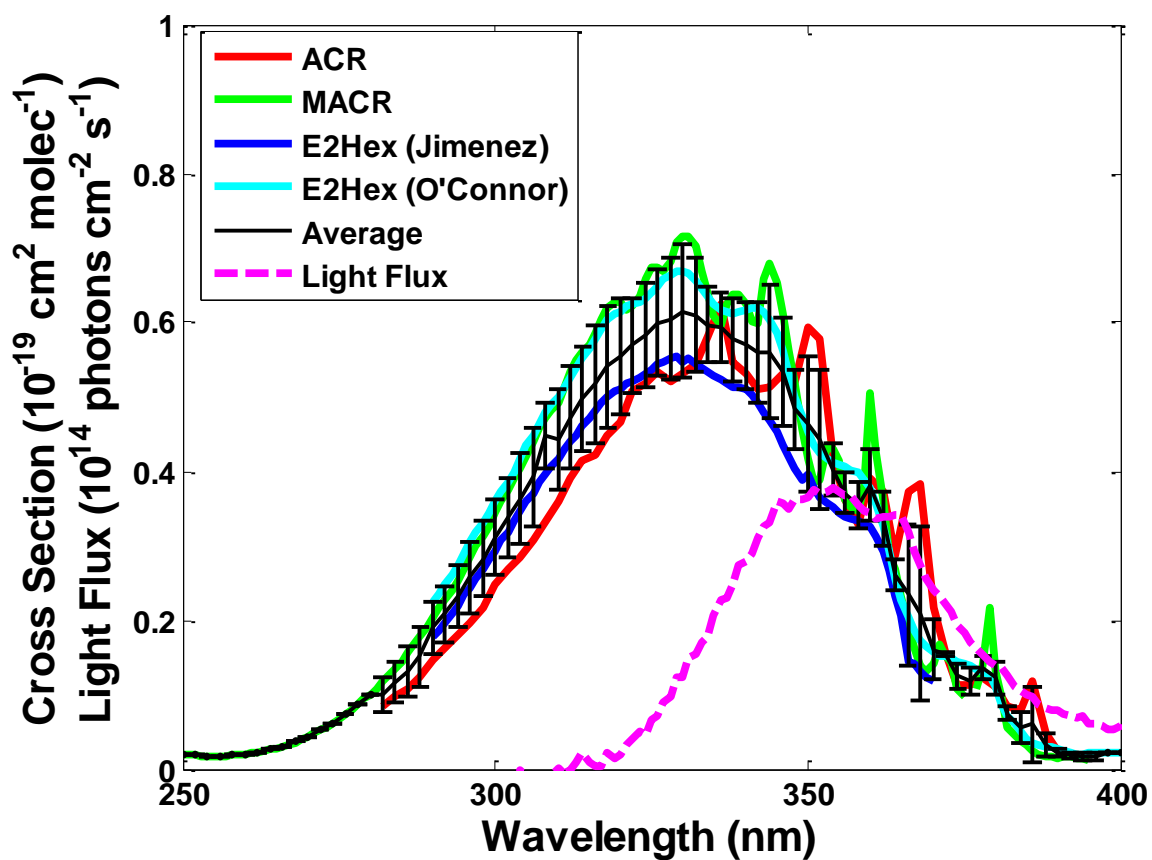
**Figure S4.** Absorption cross sections of acrolein (red), methacrolein (green) and (*E*)-2-hexenal (dark and light blue) as reported in the MPI-Mainz spectral database.[16] The two values for (*E*)-2-hexenal represent two independent studies.[14, 15] The average and standard deviation of the four values is shown in black. The measured photon flux in the reaction chamber is also shown (magenta).
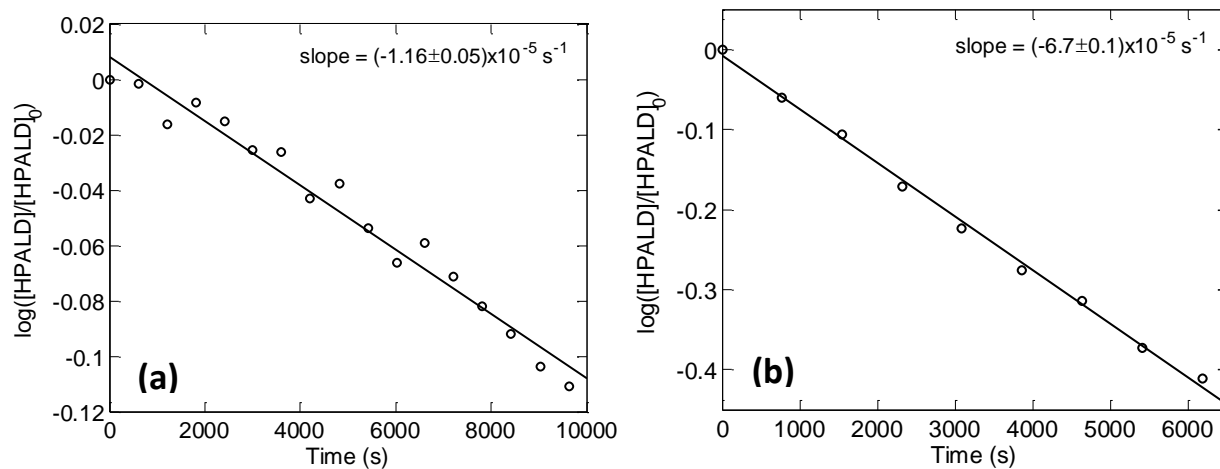
**Figure S5.** Logarithmic decay of HPALDs for ozone reaction experiments OZ1 (a) and OZ3 (b). Experiment OZ1 characterized oxidation of the $C_6$-HPALD, while OZ3 characterized oxidization of isoprene-derived $C_5$-HPALDs generated through in-chamber photochemistry prior to the experiment. Lines represent ordinary linear least-squares fits.
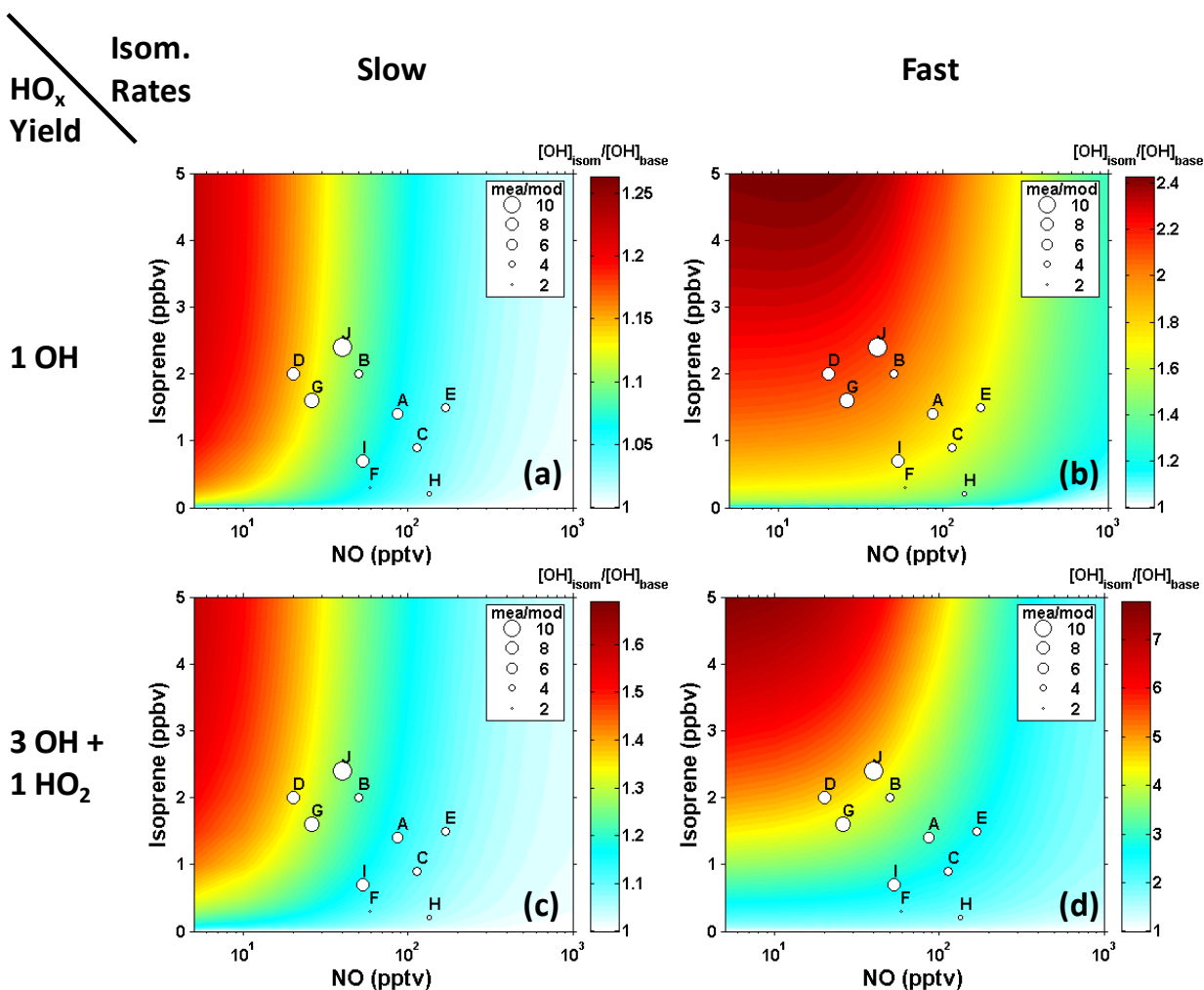
**Figure S6.** Simulated fractional change in OH concentrations in a 0-D box model resulting from the isomerization of isoprene peroxy radicals and the subsequent photolysis and OH oxidation of $C_5$-HPALDs. Model calculations use either experimental[7] ("slow") or theoretical[17] ("fast") 1,5- and 1,6-H shift isomerization rates and $C_5$-HPALD photolysis chemistry that produces either 1 OH as measured ("1 OH") or OH + $HO_2$ + PACALD and additional fast photolysis of the PACALD[17] ("3OH + 1 $HO_2$) as described in the manuscript. Note that color scales differ for each plot. Circles and corresponding letters denote chemical regimes for observational studies (Table 4). Circle sizes correspond to the ratio of measured to modeled OH.
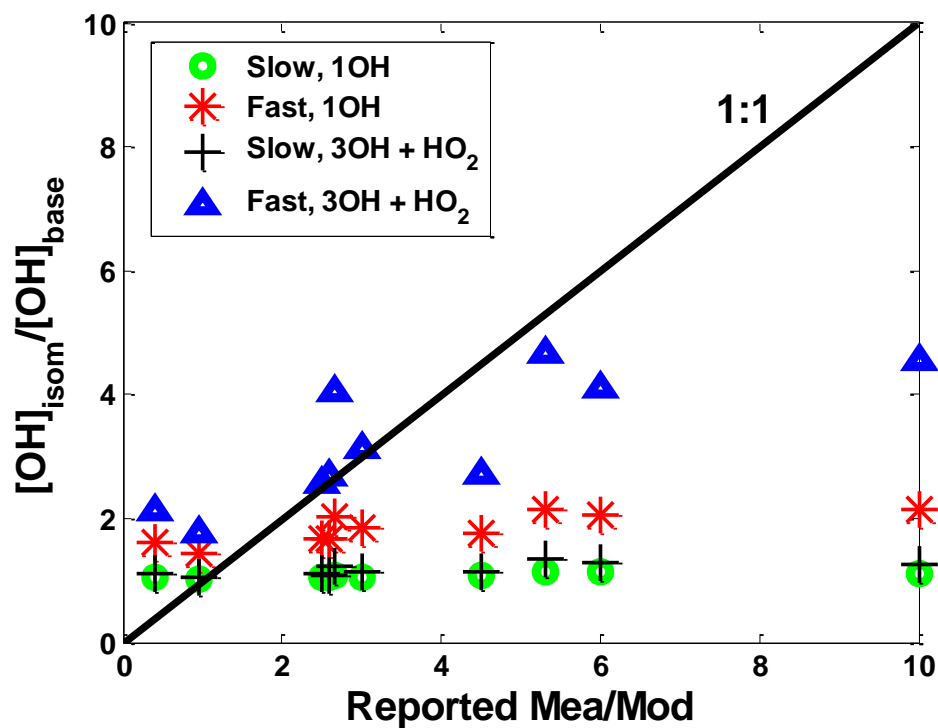
**Figure S7**. Comparison of reported ratios of measured-to-modeled OH concentrations (see Table 4 in the main text) with the modeled OH enhancement for the four scenarios shown in Fig. S6. This comparison should only be taken as approximate, as the 0-D box model was constrained with only a single set of parameters (temperature, solar zenith angle, etc.) and does not necessarily represent the actual conditions of each observation period.